ADAR1 Regulates Lipid Remodeling to Dictate Ferroptosis Sensitivity

Che-Pei Kung[1], Nick D. Terzich[2], Ma Xenia G. Ilagan[3,4], Michael J. Prinsen[3,4], Madhurima Kaushal[5], Raleigh D. Kladney[1], Jade H. Weber[1], Alex R. Mabry[1,6], Luisangely Soto Torres[1,6], Emily R. Bramel[1], Eric C. Freeman[1], Thwisha Sabloak[1], Sua Ryu[1], William M. Weber[1], Kyle A. Cottrell[7], Leonard B. Maggi Jr.[1], Leah P. Shriver[2,8,9], Gary J. Patti[2,10,11] and Jason D. Weber[1,11,12,13]

[1]Department of Medicine, Division of Molecular Oncology, Washington University School of Medicine, Saint Louis, MO, USA

[2]Department of Chemistry, Washington University, St. Louis, MO, USA

[3]High Throughput Screening Center, Washington University School of Medicine, Saint Louis, MO, USA

[4]Department of Biochemistry and Molecular Biophysics, Washington University School of Medicine, Saint Louis, MO, USA

[5]Institute for Informatics, Data Science and Biostatistics, Washington University School of Medicine, Saint Louis, MO, USA

[6]Cancer Biology Graduate Program, Washington University School of Medicine, Saint Louis, MO, USA

[7]Department of Biochemistry, Purdue University, West Lafayette, IN, USA

[8]Department of Medicine, Division of Nutritional Science and Obesity Medicine, Washington University School of Medicine, Saint Louis, MO, USA

[9]Center for Mass Spectrometry and Metabolic Tracing, Washington University, St. Louis, MO, USA

[10]Department of Genetics, Washington University, St. Louis, MO, USA

[11]Siteman Cancer Center, Washington University, St. Louis, MO, USA

[12]Department of Cell Biology and Physiology, Washington University School of Medicine, Saint Louis, MO, USA

[13]Department of Biology, Washington University, Saint Louis, MO, USA

Co-correspondence:
Che-Pei Kung, Ph.D.
Department of Medicine, Division of Molecular Oncology

Washington University School of Medicine
660 South Euclid Avenue
Campus Box 8069
St. Louis, MO 63110 USA
Email: patkung@wustl.edu
Telephone: 314-747-3898
Fax: 314-362-0152

and

Jason D. Weber, Ph.D.
Department of Medicine, Division of Molecular Oncology
Department of Cell Biology and Physiology

Washington University School of Medicine
660 South Euclid Avenue
Campus Box 8069
St. Louis, MO 63110 USA
Email: jweber@wustl.edu
Telephone: 314-747-3896
Fax: 314-362-0152

Summary

Triple-negative breast cancer (TNBC), defined by the lack of estrogen, progesterone, and HER2 receptor expressions, is aggressive and lacks targeted treatment options. Adenosine deaminase acting on RNA 1 (ADAR1) has been shown to contribute to TNBC tumorigenesis by modulating innate immune response. However, little is known about its role in regulating the metabolic fitness of TNBC. We tested the hypothesis that ferroptosis is an ADAR1-protected vulnerability by showing that ADAR1 knockdown sensitizes TNBC cells to ferroptosis inducers. Lipidomic analyses showed that ADAR1 loss increased the abundance of polyunsaturated fatty acid phospholipids, of which peroxidation is the main driver of ferroptosis. Transcriptomic analyses discovered that proto-oncogene MDM2 contributes to the lipid remodeling phenotype. A ferroptosis-focused drug screen identified FDA-approved cobimetinib as a drug-repurposing candidate to synergize with ADAR1 loss. This finding supports further basic, pre-clinical, and clinical studies to develop novel therapeutic strategies for TNBC through ADAR1-mediated metabolic regulation.

Keywords: ADAR1, RNA editing, TNBC, ferroptosis, RSL3, lipid remodeling, PUFA, MUFA, MDM2, cobimetinib.

Introduction

Despite the recent development of PARP inhibitors, immunotherapy, and antibody-drug conjugates, there remains a significant gap in targeted therapies for TNBC, contributing to its poor prognosis[1,2]. A multi-prong approach is underway to investigate the immunogenic, epigenetic, and metabolic landscapes of TNBC to identify points of vulnerability[3-5].

One such vulnerability is ferroptosis, a distinctive form of programmed cell death that depends on iron-mediated peroxidation of long polyunsaturated fatty acids (PUFA) to break down cell membranes[6]. Compared to other BC subtypes, TNBC cells express lower levels of iron exporter ferroportin, resulting in an increase of labile iron pools[7,8]. TNBC cells have also been shown to increase the uptake of cystine, a precursor for the antioxidant glutathione, rendering them more vulnerable to inhibitions of the glutamate/cystine antiporter xCT and glutathione effector GPX4[8-10]. TNBC's sensitivity to ferroptosis is also correlated with abundance of specific PUFA species, dictated by expression levels of enzymes contributing to PUFA biosynthesis, such as Acyl-CoA synthetase long-chain family member 1 and 4 (ACSL1/4), as well as fatty acid desaturases 1 and 2 (FADS1/2)[11-13].

Adenosine deaminase acting on RNA 1 (ADAR1, encoded by *ADAR*) can convert adenosine to inosine within cellular dsRNA, in a process known as A-to-I editing. Elevated expression of ADAR1 is prevalent in breast cancer and ADAR1-mediated editing has been shown to contribute to tumor progression and resistance to therapy in breast cancer, including TNBC[14-18]. We have previously reported a TNBC-centric ADAR1 dependency phenomenon, in which ADAR1 protects TNBC cells from translational stress and type I interferon activation predisposed by elevated levels of interferon stimulated gene signatures[19]. ADAR1-mediated regulation of the

innate immune response has been observed in several types of cancer, and loss of ADAR1 has been shown to sensitize certain cancers to immunotherapy[20-23]. Through its ability to prevent the cytotoxic inflammatory response, ADAR1 also protects cancer cells from other anti-tumorigenic stresses, such as necroptosis and epigenetic modulation[24,25]. However, few studies have investigated the ability of ADAR1 to regulate the metabolic fitness of cancer cells and their sensitivity to metabolic stresses. Considering the role of ADAR1 in metabolic regulation and the importance of cancer metabolism, it is important to fill these knowledge gaps[26,27].

In the current study, we demonstrate that ADAR1 protects TNBC cells from ferroptosis by regulating the expression of MDM2 and lipid profiles. Our observations indicate broader applications of ADAR1-targeting therapies against TNBC.

Results

ADAR1 protects TNBC cells from ferroptosis induction

To determine whether ADAR1 inhibits ferroptosis directly, ADAR1 was knocked down with a short hairpin RNA (shRNA) in the TNBC cell line MDA-MB-231 (**Figure S1A**). The level of malondialdehyde (MDA), a byproduct and marker of lipid peroxidation, was measured to show that cells with ADAR1 knockdown (ADAR1-deficient) did not display induced ferroptosis phenotype compared to cells treated with a non-targeting shRNA (shNT) (**Figure S1B**). Similarly, by staining both the reduced and oxidized forms of the lipid peroxidation probe BODIPY™ 581/591 C11, it was revealed that ADAR1 knockdown did not improve the cells' ability to oxidize PUFA (**Figure S1C-D**). Cell viability analysis showed that the reduced proliferation and viability of MDA-MB-231 cells resulting from ADAR1 knockdown could be partially rescued by an apoptosis inhibitor (Z-VAD-FMK) or an eIF2α inhibitor (ISRIB), but not

by ferroptosis inhibitors Ferrostatin-1 and Liproxstatin-1 (**Figure S1E**). These results suggest that depletion of ADAR1 does not overtly induce ferroptosis phenotypes.

ADAR1-intact and -deficient MDA-MB-231 cells were then tested to determine if ADAR1 expression influences cells' sensitivity to ferroptosis induction. Ferroptosis can be induced by the GPX4 inhibitor RSL3, whose effect can be rescued by the ferroptosis inhibitor Ferrostatin-1 or UAMC, but not Z-VAD-FMK or the necroptosis inhibitor Necrostatin-1 (**Figure S1F**). ADAR1-deficient cells were observed to be more sensitive to RSL3 at concentrations as low as 50nM (**Figure 1A**). A cell viability assay was performed to determine IC_{50} (half-maximal inhibitory concentration) of RSL3, and ADAR1-deficient cells (IC_{50} = 0.11μM vs 2.9μM) were 25-fold more sensitive (**Figure 1B**). A similar level of sensitization was observed when using another GPX4 inhibitor, ML162 (IC_{50} = 0.08μM vs 2.27μM) (**Figure 1C**).

To evaluate whether this sensitization effect occurs in TNBC cells in addition to MDA-MB-231, three other TNBC cell lines (MDA-MB-468, MDA-MB-436, HCC1806) were tested. In all three TNBC cell lines, ADAR1 knockdown resulted in increased RSL3 sensitivity, ranging from 3.5-fold (HCC1806) to 25-fold (MDA-MB-468) (**Figure 1D-F**). Four non-TNBC cell lines (MCF7, T47D, ZR75.1, SKBR3) were also tested. Interestingly, none of the non-TNBC cell lines acquired higher sensitivity after ADAR1 knockdown (**Figure S1G-J**). These results indicate that ADAR1 protects TNBC, but not non-TNBC, cell lines from ferroptosis induction.

An orthotopic implantation mouse model was established to test whether these *in vitro* results can be recapitulated *in vivo*. MDA-MB-231 cells stably transduced with Tet-inducible shADAR1 were implanted into the mammary fat pad of female immunocompromised NSG mice (**Figure 1G-H**). Upon the formation of palpable tumors, half of the mice were switched to a diet

containing doxycycline to induce ADAR1 knockdown (**Figure S1K**). Both control and doxycycline diet mice were subjected to i.p. injection of RSL3 (100mg/kg weight; twice a week) for 5 weeks. Weekly health and weight monitoring did not suggest additional toxicity associated with RSL3 treatment (**Figure S1L**). Doxycycline diet or RSL3 treatment alone reduced tumor burdens, and mice that received both experienced significantly slower tumor progression (**Figure 1I-K, Figure S1M-O**). Immunohistochemical staining of 4-Hydroxynonenal (4HNE), a product of lipid peroxidation, showed that the combination treatment enhanced the ferroptosis phenotype in resected tumors (**Figure 1L**). Our results suggest that ADAR1 reduction synergizes with ferroptosis induction.

Knockdown of ADAR1 leads to lipid remodeling

Multiple factors contribute to ferroptosis sensitivity, including ferrous iron availability, glutathione activity, and the relative abundance of PUFA over monounsaturated fatty acid (MUFA)[6] (**Figure 2A**). To test the hypothesis that ADAR1-deficient cells are primed for ferroptosis induction, these elements were evaluated using the MDA-MB-231 cell line as it is highly sensitized to ferroptosis induction by ADAR1 knockdown.

In ADAR1-deficient cells, both the level of total glutathione and ratio between reduced and total glutathione were unchanged (**Figure S2A-B**). FerroOrange staining was used to show that ADAR1-deficient cells do not display significantly higher levels of ferrous iron (**Figure S2C-D**). This suggests that the elevated sensitivity to ferroptosis upon ADAR1 knockdown cannot be attributed to the alteration of glutathione activity or abundance of ferrous iron.

Consequently, a lipidomic analysis was performed to identify potential changes in lipid profiles upon ADAR1 knockdown. Interestingly, a clear pattern switch was detected with the

phosphatidylcholine (PC) species, the most abundant phospholipid in mammalian cells and the most impactful phospholipid in controlling the sensitivity to ferroptosis (**Figure 2B**). The observed lipid reprogramming disproportionally enriched PC species with longer carbon chains and higher degrees of unsaturation (**Figure 2C-F**). Some of the longest and most highly unsaturated PC species, such as PC38:4, are among the most significantly enriched PCs in ADAR1-deficient cells (**Figure 2G, Figure S2E**).

To investigate whether similar lipid reprogramming occurs in TNBC cells sensitized by ADAR1 knockdown to a lesser extent, lipidomic analysis was performed with ADAR1-deficient MDA-MB-436 cells (**Figure S2F**). Several highly unsaturated PCs, such as PC 34:3, 35:3, and 44:6, were enriched after ADAR1 knockdown (**Figure 2H-I**). However, enrichment was not limited to PUFA, as some MUFA PC species (i.e. PC36:1, 37:1, 38:1) were also upregulated. Some PUFA PC species, meanwhile, appeared to be reduced (**Figure S2G**).

Interestingly, PUFAs from other phospholipid families, such as phosphatidylserine (PS) and phosphatidylethanolamine (PE), were also enriched in ADAR1-deficient MDA-MB-436 cells (**Figure 2J-L**, **Figure S2H-I**). These results showed that the reduction of ADAR1 leads to lipid remodeling, specifically enrichment of PUFA over MUFA and saturated fatty acid (SFA). Interestingly, the publicly available metabolomics dataset shows that ADAR1 expression levels strongly correlated with the abundance of SFA (PC32:0) and MUFA (PC32:1 and PC34:1) species in TNBC, but not non-TNBC cells (**Figure S2J-L**). These data support the hypothesis that in TNBC cells, ADAR1 helps maintain FA homeostasis that favors MUFA and SFA.

ADAR1 regulates MDM2 expression to dictate lipid profiles and ferroptosis sensitivity

To identify mechanisms contributing to ADAR1-regulated lipid remodeling, four TNBC cell lines (MDA-MB-231, MDA-MB-468, HCC1806, BT549) were subjected to RNA-seq analyses to compare transcriptomic profiles between ADAR1-intact and ADAR1-deficient cells (**Figure S3A, Table S1**).

Pathway analyses were performed to provide a glimpse of cellular functions impacted by ADAR1 knockdown. Genes that were altered in at least three cell lines were from a variety of pathways, including metabolic regulations in cancer cells and lipid and fatty acid metabolism (**Figure 3A-D, Figure S3B-C, Table S2-4**). Gene set enrichment analysis (GSEA) with RNA-seq data of MDA-MB-231 cells suggests that ADAR1 reduction resulted in significant changes in transcriptomes involved in fatty acid metabolism, but not in glutathione activity, iron metabolism, or direct ferroptosis regulation (**Figure 3E-F, Figure S3D-E**). The results of GSEA also suggest a lack of clear effect on interferon signaling, while the cell cycle related transcriptome was affected (**Figure S3F-G**). Interestingly, when other metabolic pathways were evaluated, ADAR1 knockdown had no effect on the glycolysis gene set, but significantly altered the transcriptome involved in amino acid metabolism (**Figure S3H-I**). This suggests that ADAR1 might affect the metabolic state of cancer cells beyond lipid programming.

To narrow down the targets for further investigation, more stringent cutoffs (FDR<0.01, Log2FC>0.5 or <-0.5) were applied to identify individual genes that were most altered. Seventeen genes (besides *ADAR*) were downregulated in at least 3 TNBC cell lines upon ADAR1 knockdown, while only one (*MDM2*) was upregulated (**Figure 3G-H**). The transcription of *MDM2* has previously been shown to be regulated by ADAR1-mediated editing[28]. The induction of MDM2 protein in ADAR1-deficient cells was confirmed in all four TNBC cell lines (**Figure 3I**, data not shown), and reduced RNA editing was observed at the

reported 3'UTR editing site using Sanger sequencing and RNA editing site-specific quantitative PCR (RESS-qPCR)[29] (**Figure 3J-K, Figure S3J-K**).

Recently MDM2 was shown to promote ferroptosis sensitivity by mediating lipid remodeling, including induction of PUFA levels[30]. To determine whether MDM2 is also capable of promoting ferroptosis sensitivity in TNBC cells, MDA-MB-231 cells overexpressing MDM2 were subjected to RSL3 treatment (**Figure 3L-M**). Overexpression of MDM2 sensitized MDA-MB-231 cells to RSL3, albeit to a lesser degree compared to ADAR1 knockdown.

To determine whether MDM2 promotes PUFA enrichment in TNBC cells, MDA-MB-231 cells possessing Tet-inducible MDM2 were subjected to lipidomic analysis to identify PC PUFA profiles at both 48 and 96 hours after doxycycline treatment (**Figure S3L**). At 48 hours, some PC PUFAs (i.e. PC34:3) were enriched (**Figure S3M**). After 96 hours, a broader enrichment profile became prominent, including inductions of several highly unsaturated PC species, such as PC42:7 and PC42:8 (**Figure 3N-O, Figure S3N**).

To confirm whether the elevated ferroptosis sensitivity after ADAR1 reduction can be attributed in fact to MDM2 induction, a rescue experiment was conducted with MDA-MB-231 cells treated with RSL3. The inflection point concentration of RSL3 (100nM) that distinguishes between ADAR1-intact and ADAR1-deficient cells was used in combination with MDM2 inhibitors. All three MDM2 inhibitors used (MX69, MEL23, SP141) partially rescued RSL3-treated ADAR1-deficient cells (**Figure 3P**). MDM2 was previously shown to promote ferroptosis sensitivity through suppressing the activity of peroxisome proliferator-activated receptor alpha (PPAR-α)[30]. Consistent with the report, an agonist of PPAR-α, pirinixic acid, was shown to confer a mild yet

significant rescue effect. These results indicate that ADAR1 regulates lipid profiles through MDM2 to protect TNBC cells from ferroptosis induction.

ADAR1 loss synergizes with cobimetinib to suppress tumorigenesis

The most widely used ferroptosis inducers in preclinical studies, such as RSL3, remain distant from clinical applications due to poor pharmacological profiles and excessive toxicity[31]. Meanwhile, many drugs currently used in clinics or tested in clinical trials possess ferroptosis-inducing activities[32]. Therefore, the opportunity exists to harness the lipid-profiling effect of ADAR1 inhibition to enhance the efficacy of treatments readily available to patients.

To identify drug candidates that synergize with ADAR1 reduction, a high-throughput screen was performed to assess the effect of ADAR1 status on the sensitivity of MDA-MB-231 cells to drugs included in a ferroptosis-focused library (**Figure 4A**). Drugs that synergize with ADAR1 reduction (ADAR1-sensitized) were expected to suppress ADAR1-deficient cells more effectively, similarly to RSL3, which was used as a positive control (**Figure 4B-C**).

Several hits were identified to react at least twice as strongly with ADAR1-deficient, compared to ADAR1-intact, cells (**Figure 4D-E**). Siramesine is a lysosome disrupting agent that induces ferroptosis by promoting reactive oxygen species (ROS) – mediated oxidative stress and reducing the expression of ferroportin-1, an iron transport protein[33,34]. SB590885 is a B-Raf inhibitor that induces the accumulation of ROS[35,36]. UC2288 is a derivative of Sorafenib, known to promote ferroptosis by regulating p21 activity[37,38]. Alpha-Mangostin is a dietary xanthone that induces ROS activity and suppresses lipogenesis[39,40]. Nordihydroguaiaretic acid (NDGA) is an inhibitor of 5-lipoxygenase (5-LOX) that promotes PUFA peroxidation[41,42]. GW284543 and

cobimetinib are both MEK inhibitors, and MEK inhibition has recently been shown to induce ferroptosis in lung and ovarian cancers[43,44].

Among the identified hits, cobimetinib is the only FDA-approved drug. Currently, cobimetinib is approved for the treatment of metastatic melanoma and histiocytic neoplasms but was also shown to improve the survival of TNBC patients when combined with chemotherapy and immunotherapy[45-47]. Publicly available drug response data show that cobimetinib exhibits stronger activity toward TNBC compared to non-TNBC cell lines, similar to carboplatin, which is known to improve the outcome of TNBC[48] (**Figure S4A-B**).

The orthotopic implantation mouse model described earlier was used to test the synergistic effect between ADAR1 reduction and cobimetinib *in vivo* (**Figure S4C**). Upon the formation of palpable tumors from MDA-MB-231 cells, mice were fed a control diet or a diet containing doxycycline to induce ADAR1 knockdown before being subjected to cobimetinib treatment (oral administration at 20mg/kg weight; twice a week) for 5 weeks. The combination of the doxycycline diet and cobimetinib showed superior tumor suppressive efficacy without noted toxicity, indicating a strong synergy between ADAR1 reduction and cobimetinib (**Figure 4F-H, Figure S4D-G**).

Discussion

Justified by the data shown in this study, we expanded our knowledge of ADAR1-associated vulnerabilities in TNBC by showing that ADAR1 depletion sensitizes TNBC cells to ferroptosis induction. Two recent studies showed that ADAR1 loss leads to overt ferroptosis phenotypes[49,50]. Different experimental conditions are known to affect ferroptosis phenotypes[51,52]. In particular, CRISPR (clustered regularly interspaced short palindromic repeats) – mediated gene editing used

to knock out ADAR1 in these studies has been shown to alter the p53 signaling pathway, which can promote ferroptosis[53,54]. Despite the disparate observations, our results agree with the premise that ADAR1 plays a protective role against ferroptosis.

ADAR1-mediated desensitization to ferroptosis was attributed to lipid remodeling, as the reduction of ADAR1 led to increased PUFA abundance. Transcriptomic analysis revealed that MDM2 is one of the commonly regulated genes in ADAR1-deficient TNBC cell lines that are sensitized to ferroptosis. Consistent with its reported function in promoting ferroptosis through lipid reprogramming, MDM2 expression and activity were shown to be related to ADAR1-regulated ferroptosis sensitivity[30]. These results reveal a novel mechanism by which ADAR1 protects TNBC cells from stresses that could lead to ferroptosis (**Figure 4I**).

Surprisingly, publicly available drug response data show that the sensitivity of TNBC cells to the three ferroptosis inducers used in this study (RSL3, ML162, cobimetinib) is inversely correlated with their dependence on ADAR1 (**Figure S4H-J**). This suggests that the dependence of TNBC cells on ADAR1 could be partially attributed to its ferroptosis-protecting activity. Although recent studies have questioned ADAR1's status as a *bona fide* oncogene, it deserves to be considered a critical non-oncogene target for its ability to suppress multiple stresses directly and indirectly[55,56]. The lack of ferroptosis with ADAR1 knockdown alone suggests that observed MDM2-mediated lipid remodeling serves as a priming event for ferroptosis inducers. Supporting the potential of this approach, recent studies revealed that TNBC cells are protected from ferroptosis by MUFAs generated both intracellularly and by their originating environment[57-59].

Preliminary results showed that non-TNBC cells with ADAR1 knockdown are not sensitized to RSL3. Multiple mechanisms contribute to ferroptosis resistance in non-TNBC cells, suggesting

higher thresholds for sensitization[60-64]. It is worth noting that TNBCs disproportionally possess deactivating p53 mutations that abrogate MDM2 interactions[65]. Therefore, the ability of MDM2 to promote lipid remodeling and ferroptosis sensitivity could be dictated by its dynamic relationship with p53. The recent discovery of the role of mutant p53 in protecting TNBC from ferroptosis indicates that MDM2 plays an antagonistic role in promoting ferroptosis sensitivity[66]. With its many p53-independent functions, both pro- and anti-tumorigenic, the complex role of MDM2 in the ADAR1 targeting strategy against TNBC warrants further investigation[67,68].

Exciting opportunities are highlighted by the synergistic effect between reduced ADAR1 expression and ferroptosis. In addition to the lack of clinically proven ADAR1 and ferroptosis modulators, both ADAR1 inactivation and ferroptosis have been associated with pathological consequences[31,69,70]. In addition to developing effective ADAR1 inhibitors, functional drug repurposing offers a derisking strategy[70,71]. A ferroptosis-focused screen identified cobimetinib, an FDA-approved MEK inhibitor with ferroptosis-inducing activity, to be sensitized with ADAR1 loss. Cobimetinib and other MEK inhibitors have been shown in preclinical and clinical settings to inhibit TNBC tumorigenesis[47,72]. Cobimetinib has also been shown to induce a type I interferon response, indicating the potential of repurposing drugs that impact multiple pathways downstream of ADAR1[73]. Future studies could examine if other existing TNBC treatments, such as platinum-based agents, also synergize with ADAR1 inhibition with their ferroptosis-promoting activity[74].

Results shown in our study raise several questions about the implication of ADAR1's ability to regulate lipid metabolism and ferroptosis sensitivity. Does ADAR1 expression or its editing profile have a prognostic value, like the recently shown androgen receptor, to predict the response of patients with TNBC to ferroptosis inducers[75]? As both ferroptosis and ADAR1

inhibition can sensitize 'immune cold' tumors to immunotherapy, can a sequential or combined approach targeting ADAR1, ferroptosis, and immune checkpoints minimize resistance to treatment[76,77]? Does ADAR1 protect TNBC from other metabolic stresses, such as amino acid dysregulation[27]? And how do ADAR1-regulated metabolic adaptations fit into dietary interventions to improve cancer treatment[78-80]? ADAR1 is capable of altering most RNA species and has immense potential for exploitation to develop innovative therapies against challenging cancers such as TNBC.

Resource availability

Lead contact

Requests for further information and resources should be directed to and will be fulfilled by the lead contact, Jason D. Weber (jweber@wustl.edu).

Materials availability

All unique/stable reagents generated in this study are available from the lead contact with a completed materials transfer agreement.

Data and code availability

All data reported in this paper will be shared by the lead contact upon request. This paper does not report original code. Any additional information required to reanalyze the data reported in this paper is available from the lead contact upon request.

Acknowledgements

We thank the Division of Comparative Medicine at Washington University in St. Louis for housing the mouse colony. We thank the Denardo lab for processing the fixed tumor tissues. We thank the Tissue Histology Core, Department of Obstetrics and Gynecology, for sectioning the

tumor samples and performing H&E staining. We thank the support by the Genome Technology Access Center (GTAC) at McDonnell Genome Institute (MGI) Symposium Pilot Project Funding to perform RNA-seq analyses (Catrina Fronick and Michael Heinz for logistics; Toni Sinnwell, Elliott Klotz, and Eric Tycksen for quality control, sequencing and analyses). We acknowledge the Just-In-Time (JIT) Core Usage Funding Program to support the collaboration with HTSC for drug screening. Both GTAC@MGI Symposium Pilot Project and JIT programs are funded through the Institute of Clinical and Translational Sciences (ICTS), Washington University in St. Louis. ICTS was supported by the National Center for Advancing Translational Sciences (NCATS) grant UL1TR002345. This work was supported by R01CA262804 (JDW) from National Cancer Institute (NCI), and W81XWH-21-1-0476 and W81XWH-21-1-0466 from the Congressionally Directed Medical Research Programs (CDMRP), Department of Defense (JDW). C-P. K received support from Transdisciplinary Research in Energetics and Cancer (TREC) Training Workshop R25CA203650 from NCI and TL1 Translational Sciences Postdoctoral Program TL1TR002344 from National Center for Advancing Translational Sciences. L.S.T. is supported by R25HG006687 and T32GM148405 from National Human Genome Research Institute and National Institute of General Medical Sciences, respectively.

Author contributions

C-P. Kung: Conceptualization, investigation, methodology, formal analysis, project administration, writing–original draft, writing–review and editing. **N.D. Terzich:** investigation, methodology, formal analysis. **M.X.G. Ilagan:** investigation, methodology, formal analysis, writing–review and editing. **M.J. Prinsen:** Investigation, methodology, formal analysis. **M. Kaushal:** Investigation, methodology, formal analysis. **R.D. Kladney:** Investigation, methodology. **J.H. Weber:** Investigation. **A.R. Mabry:** Investigation. **L.S. Torres:**

Investigation. **E.R. Bramel:** Investigation. **E.C. Freeman:** Investigation. **T. Sabloak:** Investigation. **K.A. Cottrell:** Investigation. **S. Ryu:** Investigation. **W.M. Weber:** Investigation. **L.B. Maggi Jr.:** investigation, writing–review and editing. **L.P. Shriver:** investigation, methodology, writing–review and editing. **G.J. Patti:** funding acquisition, investigation, writing–review and editing. **J.D. Weber:** Conceptualization, resources, supervision, funding acquisition, writing–original draft, writing–review and editing.

Declaration of interests

G.J. Patti is the Chief Scientific Officer of Panome Bio, a scientific advisory board member for Cambridge Isotope Laboratories, and has a collaborative research agreement with Agilent Technologies.

Supplemental information

Document S1. Figure S1-S4

Table S1. Genes altered in ADAR1-deficient TNBC cell lines, related to Figure 3

Table S2. Signaling pathways altered upon ADAR1 knockdown, related to Figure 3

Table S3. Disease-related biological functions altered upon ADAR1 knockdown, related to Figure 3

Table S4. Biological pathways altered upon ADAR1 knockdown, related to Figure S3

Figure 1. ADAR1 protects TNBC cells from ferroptosis induction

A) Light micrographs of ADAR1-intact (shNT) and -deficient (shADAR1) MDA-MB-231 cells treated with RSL3 for 24h. Cell viability analyses were performed to determine IC_{50} values of ferroptosis inducers **B)** RSL3 and **C)** ML162 for MDA-MB-231 cells. IC_{50} of RSL3 were determined for **D)** MDA-MB-436, **E)** HCC1806, and **F)** MDA-MB-468 TNBC cells. Cell viability graphs are representatives of three replicates. FC, fold-change. **G)** Immunoblot analysis showed similar levels of ADAR1 knockdown in doxycycline-treated MDA-MB-231 cells with Tet-inducible shADAR1 compared to cells treated with shADAR1-containing lentivirus. Images are representative of three replicates. GAPDH, loading control. **H)** MDA-MB-231 cells (1.5 X 10^5 per mouse) with Tet-inducible shADAR1 were implanted into mammary fat pads of female mice. Ten days post implantation, half of the mice were switched to doxycycline-containing (625mg/kg) diet, followed by RSL3 treatments (100mg/kg weight; i.p. injection twice a week) for 5 weeks. **I)** Progression of overall tumor volumes, n=5-9 each group. Error bars mark standard deviation. **J)** Quantification of areas under curve (AUC) from I). Error bars mark standard deviation. **K)** Two-way ANOVA analysis to compare weekly measured overall tumor volumes. Statistically significant p-values (<0.05) were highlighted in red. **L)** Representative images of IHC staining of H&E, ADAR1 (p150 isoform), and 4HNE in resected tumor samples. Scale bar, 200µm. See also **Figure S1**.

Figure 2: ADAR1 reduction leads to lipid remodeling

A) Key regulators of ferroptosis. GSH, Glutathione. PL, phospholipid. MUFA, monounsaturated fatty acid. PUFA, polyunsaturated fatty acid. PM, plasma membrane. **B)** Heatmap of lipidomic analysis in MDA-MB-231 cells upon ADAR1 knockdown. PC, phosphatidylcholines. **C)** Relative abundance of PC species listed in the order of carbon chain length or **D)** lipid unsaturation. Values were log10 transformed, mean centered, and shown as mean over standard deviation ratio. n=5. Red dots denote ADAR1-intact, and blue dots denote ADAR1-deficient samples. **E)** Enrichment of PC species with different carbon chain lengths and **F)** different unsaturation levels (SFA, 0 double-bond; MUFA, 1 double-bond; PUFA, ≥ 2 double-bond; XPUFA, ≥ 4 double-bond) upon ADAR1 knockdown. Data from individual samples (n=4) were normalized to the average intensity in shNT samples. **G)** Relative abundance of PC38:4 between ADAR1-intact and -deficient MDA-MB-231 cells. Data from individual samples (n=5) were divided by the overall average of PC38:4 intensity in all samples and log2 transformed. **H)** Relative abundance of selected PC species in ADAR1-intact and -deficient MDA-MB-436 cells. n=3. **I)** Relative abundance of PC44:6 in MDA-MB-436 cells. n=3. **J)** Relative abundance of PE and PS species in ADAR1-intact and -deficient MDA-MB-436 cells, listed in the order of lipid unsaturation. n=3. **K)** Enrichment of PE and PS species with different unsaturation levels (MUFA, 1 double-bond; PUFA, ≥ 2 double-bond; XPUFA, ≥ 5 double-bond) upon ADAR1 knockdown in MDA-MB-436 cells. n=3. **L)** Relative abundance of PE38:5 in MDA-MB-436 cells. n=3. See also **Figure S2**.

Figure 3: ADAR1 regulates MDM2 expression to dictate ferroptosis sensitivity

A) Downregulated and **B)** upregulated genes ($p<0.05$) in ADAR1-deficient TNBC cell lines. **C)** Significantly altered signaling pathways (BioPlanet_2019) and **D)** disease-related biological functions (PheWeb_2019) in ADAR1-deficient TNBC cells. Genes altered in at least 3 cell lines are included. **E)** GSEA enrichment plot of ferroptosis and **F)** fatty acid metabolism genes in ADAR1-deficient MDA-MB-231 cells. **G)** The most significantly downregulated and **H)** upregulated genes (FDR<0.01, Log2FC<-0.5 or >0.5) in ADAR1-deficient TNBC cells. Genes altered in at least 3 cell lines are listed on the right. **I)** Immunoblot analysis showed MDM2 induction upon ADAR1 knockdown in MDA-MB-231 cells. Images are representative of three replicates. GAPDH, loading control. **J)** Reported ADAR1 editing site (bolded and underlined) in MDM2 3'UTR. Numbers mark the location within the open reading frame. **K)** RESS-qPCR showed reduced editing of MDM2 3'UTR site in ADAR1-deficient cells. n=3. Error bars mark standard error. **L)** Immunoblot analysis showed MDM2 (Myc-tagged) overexpression in MDA-MB-231 cells. GAPDH, loading control. **M)** IC_{50} of RSL3 for MDA-MB-231 cells with MDM2 overexpression. Graph is representative of three replicates. FC, fold-change. **N)** Relative abundance of PUFA PC species, listed in the order of lipid unsaturation, in MDA-MB-231 cells with MDM2 overexpression (red dots) for 96 h. n=5. **O)** Relative abundance of PC42:7 between control (Ctrl) and MDM2-overexpressing MDA-MB-231 cells. n=5. **P)** Relative cell viability within ADAR1-intact and -deficient MDA-MB-231 cells treated with RSL3 (100nM), as well as ADAR1-deficient cells co-treated with MDM2 inhibitors MX69 (10µM), MEL23 (10µM), and SP-141 (10µM), or PPAR-α agonist pirinixic acid (PA; 10µM) for 72h. n=3. Error bars mark standard error. See also **Figure S3 and Table S1-4**.

Figure 4: ADAR1 loss synergizes with cobimetinib to suppress tumorigenesis

A) Drug screen to identify ADAR1-sensitized ferroptosis modulators. **B)** ADAR1-sensitized hits (red dots) preferentially reduce viability of ADAR1-deficient cells. X and Y axis represent cell viability for ADAR1-intact and -deficient cells, respectively. **C)** Screening result with a ferroptosis-focused library (654 small molecules) in MDA-MB-231 cells. Data were normalized to DMSO-treated cells. RSL3 was included as positive control. Dashed line denotes expected locations for molecules without discriminating activity. **D)** Cell viability ratio of 0.51 (horizontal red line) between ADAR1-deficient and -Intact cells (shADAR1/shNT) was used as the cutoff to identify ADAR1-sensitized hits. **E)** List of hits identified, ranked by cell viability ratio. **F)** Progression of overall tumor volumes, n=5-10 each group. Error bars mark standard deviation. **G)** Quantification of areas under curve (AUC) from F). Error bars mark standard deviation. **H)** Two-way ANOVA analysis to compare weekly measured overall tumor volumes. Statistically significant p-values (<0.05) were highlighted in red. **I)** ADAR1 protects TNBC cells from ferroptosis through regulating MDM2 and lipid compositions between MUFA and PUFA. FIN, ferroptosis inducer. See also **Figure S4**.

References

1. Obidiro, O., Battogtokh, G., and Akala, E.O. (2023). Triple Negative Breast Cancer Treatment Options and Limitations: Future Outlook. Pharmaceutics *15*. 10.3390/pharmaceutics15071796.
2. Ademuyiwa, F.O., Tao, Y., Luo, J., Weilbaecher, K., and Ma, C.X. (2017). Differences in the mutational landscape of triple-negative breast cancer in African Americans and Caucasians. Breast Cancer Res Treat *161*, 491-499. 10.1007/s10549-016-4062-y.
3. Loizides, S., and Constantinidou, A. (2022). Triple negative breast cancer: Immunogenicity, tumor microenvironment, and immunotherapy. Front Genet *13*, 1095839. 10.3389/fgene.2022.1095839.
4. Zhou, L., and Yu, C.W. (2024). Epigenetic modulations in triple-negative breast cancer: Therapeutic implications for tumor microenvironment. Pharmacol Res *204*, 107205. 10.1016/j.phrs.2024.107205.
5. Munkacsy, G., Santarpia, L., and Gyorffy, B. (2023). Therapeutic Potential of Tumor Metabolic Reprogramming in Triple-Negative Breast Cancer. Int J Mol Sci *24*. 10.3390/ijms24086945.
6. Stockwell, B.R. (2022). Ferroptosis turns 10: Emerging mechanisms, physiological functions, and therapeutic applications. Cell *185*, 2401-2421. 10.1016/j.cell.2022.06.003.
7. Pinnix, Z.K., Miller, L.D., Wang, W., D'Agostino, R., Jr., Kute, T., Willingham, M.C., Hatcher, H., Tesfay, L., Sui, G., Di, X., et al. (2010). Ferroportin and iron regulation in breast cancer progression and prognosis. Sci Transl Med *2*, 43ra56. 10.1126/scitranslmed.3001127.
8. Verma, N., Vinik, Y., Saroha, A., Nair, N.U., Ruppin, E., Mills, G., Karn, T., Dubey, V., Khera, L., Raj, H., et al. (2020). Synthetic lethal combination targeting BET uncovered intrinsic susceptibility of TNBC to ferroptosis. Sci Adv *6*. 10.1126/sciadv.aba8968.
9. Beatty, A., Fink, L.S., Singh, T., Strigun, A., Peter, E., Ferrer, C.M., Nicolas, E., Cai, K.Q., Moran, T.P., Reginato, M.J., et al. (2018). Metabolite Profiling Reveals the Glutathione Biosynthetic Pathway as a Therapeutic Target in Triple-Negative Breast Cancer. Mol Cancer Ther *17*, 264-275. 10.1158/1535-7163.MCT-17-0407.
10. Timmerman, L.A., Holton, T., Yuneva, M., Louie, R.J., Padro, M., Daemen, A., Hu, M., Chan, D.A., Ethier, S.P., van 't Veer, L.J., et al. (2013). Glutamine sensitivity analysis identifies the xCT antiporter as a common triple-negative breast tumor therapeutic target. Cancer Cell *24*, 450-465. 10.1016/j.ccr.2013.08.020.
11. Beatty, A., Singh, T., Tyurina, Y.Y., Tyurin, V.A., Samovich, S., Nicolas, E., Maslar, K., Zhou, Y., Cai, K.Q., Tan, Y., et al. (2021). Ferroptotic cell death triggered by conjugated linolenic acids is mediated by ACSL1. Nat Commun *12*, 2244. 10.1038/s41467-021-22471-y.
12. Lorito, N., Subbiani, A., Smiriglia, A., Bacci, M., Bonechi, F., Tronci, L., Romano, E., Corrado, A., Longo, D.L., Iozzo, M., et al. (2024). FADS1/2 control lipid metabolism and ferroptosis susceptibility in triple-negative breast cancer. EMBO Mol Med *16*, 1533-1559. 10.1038/s44321-024-00090-6.
13. Doll, S., Proneth, B., Tyurina, Y.Y., Panzilius, E., Kobayashi, S., Ingold, I., Irmler, M., Beckers, J., Aichler, M., Walch, A., et al. (2017). ACSL4 dictates ferroptosis sensitivity by shaping cellular lipid composition. Nat Chem Biol *13*, 91-98. 10.1038/nchembio.2239.
14. Fumagalli, D., Gacquer, D., Rothe, F., Lefort, A., Libert, F., Brown, D., Kheddoumi, N., Shlien, A., Konopka, T., Salgado, R., et al. (2015). Principles Governing A-to-I RNA

Editing in the Breast Cancer Transcriptome. Cell Rep *13*, 277-289. 10.1016/j.celrep.2015.09.032.

15. Peng, X., Xu, X., Wang, Y., Hawke, D.H., Yu, S., Han, L., Zhou, Z., Mojumdar, K., Jeong, K.J., Labrie, M., et al. (2018). A-to-I RNA Editing Contributes to Proteomic Diversity in Cancer. Cancer Cell *33*, 817-828 e817. 10.1016/j.ccell.2018.03.026.
16. Han, L., Diao, L., Yu, S., Xu, X., Li, J., Zhang, R., Yang, Y., Werner, H.M.J., Eterovic, A.K., Yuan, Y., et al. (2015). The Genomic Landscape and Clinical Relevance of A-to-I RNA Editing in Human Cancers. Cancer Cell *28*, 515-528. 10.1016/j.ccell.2015.08.013.
17. Paz-Yaacov, N., Bazak, L., Buchumenski, I., Porath, H.T., Danan-Gotthold, M., Knisbacher, B.A., Eisenberg, E., and Levanon, E.Y. (2015). Elevated RNA Editing Activity Is a Major Contributor to Transcriptomic Diversity in Tumors. Cell Rep *13*, 267-276. 10.1016/j.celrep.2015.08.080.
18. Baker, A.R., Miliotis, C., Ramirez-Moya, J., Marc, T., Vlachos, I.S., Santisteban, P., and Slack, F.J. (2022). Transcriptome Profiling of ADAR1 Targets in Triple-Negative Breast Cancer Cells Reveals Mechanisms for Regulating Growth and Invasion. Mol Cancer Res *20*, 960-971. 10.1158/1541-7786.MCR-21-0604.
19. Kung, C.P., Cottrell, K.A., Ryu, S., Bramel, E.R., Kladney, R.D., Bao, E.A., Freeman, E.C., Sabloak, T., Maggi, L., Jr., and Weber, J.D. (2021). Evaluating the therapeutic potential of ADAR1 inhibition for triple-negative breast cancer. Oncogene *40*, 189-202. 10.1038/s41388-020-01515-5.
20. Karki, R., Sundaram, B., Sharma, B.R., Lee, S., Malireddi, R.K.S., Nguyen, L.N., Christgen, S., Zheng, M., Wang, Y., Samir, P., et al. (2021). ADAR1 restricts ZBP1-mediated immune response and PANoptosis to promote tumorigenesis. Cell Rep *37*, 109858. 10.1016/j.celrep.2021.109858.
21. Liu, H., Golji, J., Brodeur, L.K., Chung, F.S., Chen, J.T., deBeaumont, R.S., Bullock, C.P., Jones, M.D., Kerr, G., Li, L., et al. (2019). Tumor-derived IFN triggers chronic pathway agonism and sensitivity to ADAR loss. Nat Med *25*, 95-102. 10.1038/s41591-018-0302-5.
22. Ishizuka, J.J., Manguso, R.T., Cheruiyot, C.K., Bi, K., Panda, A., Iracheta-Vellve, A., Miller, B.C., Du, P.P., Yates, K.B., Dubrot, J., et al. (2019). Loss of ADAR1 in tumours overcomes resistance to immune checkpoint blockade. Nature *565*, 43-48. 10.1038/s41586-018-0768-9.
23. Gannon, H.S., Zou, T., Kiessling, M.K., Gao, G.F., Cai, D., Choi, P.S., Ivan, A.P., Buchumenski, I., Berger, A.C., Goldstein, J.T., et al. (2018). Identification of ADAR1 adenosine deaminase dependency in a subset of cancer cells. Nat Commun *9*, 5450. 10.1038/s41467-018-07824-4.
24. Zhang, T., Yin, C., Fedorov, A., Qiao, L., Bao, H., Beknazarov, N., Wang, S., Gautam, A., Williams, R.M., Crawford, J.C., et al. (2022). ADAR1 masks the cancer immunotherapeutic promise of ZBP1-driven necroptosis. Nature *606*, 594-602. 10.1038/s41586-022-04753-7.
25. Mehdipour, P., Marhon, S.A., Ettayebi, I., Chakravarthy, A., Hosseini, A., Wang, Y., de Castro, F.A., Loo Yau, H., Ishak, C., Abelson, S., et al. (2020). Epigenetic therapy induces transcription of inverted SINEs and ADAR1 dependency. Nature *588*, 169-173. 10.1038/s41586-020-2844-1.
26. McGuirk, S., Audet-Delage, Y., and St-Pierre, J. (2020). Metabolic Fitness and Plasticity in Cancer Progression. Trends Cancer *6*, 49-61. 10.1016/j.trecan.2019.11.009.

27. Kung, C.P., Maggi, L.B., Jr., and Weber, J.D. (2018). The Role of RNA Editing in Cancer Development and Metabolic Disorders. Front Endocrinol (Lausanne) *9*, 762. 10.3389/fendo.2018.00762.
28. Yang, C.C., Chen, Y.T., Chang, Y.F., Liu, H., Kuo, Y.P., Shih, C.T., Liao, W.C., Chen, H.W., Tsai, W.S., and Tan, B.C. (2017). ADAR1-mediated 3' UTR editing and expression control of antiapoptosis genes fine-tunes cellular apoptosis response. Cell Death Dis *8*, e2833. 10.1038/cddis.2017.12.
29. Crews, L.A., Jiang, Q., Zipeto, M.A., Lazzari, E., Court, A.C., Ali, S., Barrett, C.L., Frazer, K.A., and Jamieson, C.H. (2015). An RNA editing fingerprint of cancer stem cell reprogramming. J Transl Med *13*, 52. 10.1186/s12967-014-0370-3.
30. Venkatesh, D., O'Brien, N.A., Zandkarimi, F., Tong, D.R., Stokes, M.E., Dunn, D.E., Kengmana, E.S., Aron, A.T., Klein, A.M., Csuka, J.M., et al. (2020). MDM2 and MDMX promote ferroptosis by PPARalpha-mediated lipid remodeling. Genes Dev *34*, 526-543. 10.1101/gad.334219.119.
31. Liu, J., Kang, R., and Tang, D. (2024). Adverse effects of ferroptotic therapy: mechanisms and management. Trends Cancer *10*, 417-429. 10.1016/j.trecan.2024.01.002.
32. Zhao, L., Zhou, X., Xie, F., Zhang, L., Yan, H., Huang, J., Zhang, C., Zhou, F., Chen, J., and Zhang, L. (2022). Ferroptosis in cancer and cancer immunotherapy. Cancer Commun (Lond) *42*, 88-116. 10.1002/cac2.12250.
33. Ma, S., Henson, E.S., Chen, Y., and Gibson, S.B. (2016). Ferroptosis is induced following siramesine and lapatinib treatment of breast cancer cells. Cell Death Dis *7*, e2307. 10.1038/cddis.2016.208.
34. Ostenfeld, M.S., Fehrenbacher, N., Hoyer-Hansen, M., Thomsen, C., Farkas, T., and Jaattela, M. (2005). Effective tumor cell death by sigma-2 receptor ligand siramesine involves lysosomal leakage and oxidative stress. Cancer Res *65*, 8975-8983. 10.1158/0008-5472.CAN-05-0269.
35. Gagliardi, M., Cotella, D., Santoro, C., Cora, D., Barlev, N.A., Piacentini, M., and Corazzari, M. (2019). Aldo-keto reductases protect metastatic melanoma from ER stress-independent ferroptosis. Cell Death Dis *10*, 902. 10.1038/s41419-019-2143-7.
36. Haq, R., Shoag, J., Andreu-Perez, P., Yokoyama, S., Edelman, H., Rowe, G.C., Frederick, D.T., Hurley, A.D., Nellore, A., Kung, A.L., et al. (2013). Oncogenic BRAF regulates oxidative metabolism via PGC1alpha and MITF. Cancer Cell *23*, 302-315. 10.1016/j.ccr.2013.02.003.
37. Gao, F., Zhang, B., Sun, Z., Gao, Y., Liu, C., Dou, X., Tong, H., and Wang, R. (2023). Regulation of endothelial ferroptosis by SESN1 in atherosclerosis and its related mechanism. Aging (Albany NY) *15*, 5052-5065. 10.18632/aging.204777.
38. Dixon, S.J., Patel, D.N., Welsch, M., Skouta, R., Lee, E.D., Hayano, M., Thomas, A.G., Gleason, C.E., Tatonetti, N.P., Slusher, B.S., and Stockwell, B.R. (2014). Pharmacological inhibition of cystine-glutamate exchange induces endoplasmic reticulum stress and ferroptosis. Elife *3*, e02523. 10.7554/eLife.02523.
39. Lee, C.H., Ying, T.H., Chiou, H.L., Hsieh, S.C., Wen, S.H., Chou, R.H., and Hsieh, Y.H. (2017). Alpha-mangostin induces apoptosis through activation of reactive oxygen species and ASK1/p38 signaling pathway in cervical cancer cells. Oncotarget *8*, 47425-47439. 10.18632/oncotarget.17659.
40. Shi, Y., Fan, Y., Hu, Y., Jing, J., Wang, C., Wu, Y., Geng, Q., Dong, X., Li, E., and Dong, D. (2020). alpha-Mangostin suppresses the de novo lipogenesis and enhances the

chemotherapeutic response to gemcitabine in gallbladder carcinoma cells via targeting the AMPK/SREBP1 cascades. J Cell Mol Med *24*, 760-771. 10.1111/jcmm.14785.

41. Gilbert, N.C., Gerstmeier, J., Schexnaydre, E.E., Borner, F., Garscha, U., Neau, D.B., Werz, O., and Newcomer, M.E. (2020). Structural and mechanistic insights into 5-lipoxygenase inhibition by natural products. Nat Chem Biol *16*, 783-790. 10.1038/s41589-020-0544-7.
42. Sun, Q.Y., Zhou, H.H., and Mao, X.Y. (2019). Emerging Roles of 5-Lipoxygenase Phosphorylation in Inflammation and Cell Death. Oxid Med Cell Longev *2019*, 2749173. 10.1155/2019/2749173.
43. Bhatt, V., Lan, T., Wang, W., Kong, J., Lopes, E.C., Wang, J., Khayati, K., Raju, A., Rangel, M., Lopez, E., et al. (2023). Inhibition of autophagy and MEK promotes ferroptosis in Lkb1-deficient Kras-driven lung tumors. Cell Death Dis *14*, 61. 10.1038/s41419-023-05592-8.
44. Yin, J., Chen, J., Hong, J.H., Huang, Y., Xiao, R., Liu, S., Deng, P., Sun, Y., Chai, K.X.Y., Zeng, X., et al. (2024). 4EBP1-mediated SLC7A11 protein synthesis restrains ferroptosis triggered by MEK inhibitors in advanced ovarian cancer. JCI Insight *9*. 10.1172/jci.insight.177857.
45. Larkin, J., Ascierto, P.A., Dreno, B., Atkinson, V., Liszkay, G., Maio, M., Mandala, M., Demidov, L., Stroyakovskiy, D., Thomas, L., et al. (2014). Combined vemurafenib and cobimetinib in BRAF-mutated melanoma. N Engl J Med *371*, 1867-1876. 10.1056/NEJMoa1408868.
46. Diamond, E.L., Durham, B.H., Ulaner, G.A., Drill, E., Buthorn, J., Ki, M., Bitner, L., Cho, H., Young, R.J., Francis, J.H., et al. (2019). Efficacy of MEK inhibition in patients with histiocytic neoplasms. Nature *567*, 521-524. 10.1038/s41586-019-1012-y.
47. Brufsky, A., Kim, S.B., Zvirbule, Z., Eniu, A., Mebis, J., Sohn, J.H., Wongchenko, M., Chohan, S., Amin, R., Yan, Y., et al. (2021). A phase II randomized trial of cobimetinib plus chemotherapy, with or without atezolizumab, as first-line treatment for patients with locally advanced or metastatic triple-negative breast cancer (COLET): primary analysis. Ann Oncol *32*, 652-660. 10.1016/j.annonc.2021.01.065.
48. Han, H.S., Vikas, P., Costa, R.L.B., Jahan, N., Taye, A., and Stringer-Reasor, E.M. (2023). Early-Stage Triple-Negative Breast Cancer Journey: Beginning, End, and Everything in Between. Am Soc Clin Oncol Educ Book *43*, e390464. 10.1200/EDBK_390464.
49. Yin, C., Zhang, M.M., Wang, G.L., Deng, X.Y., Tu, Z., Jiang, S.S., Gao, Z.D., Hao, M., Chen, Y., Li, Y., and Yang, S.Y. (2024). Loss of ADAR1 induces ferroptosis of breast cancer cells. Cell Signal *121*, 111258. 10.1016/j.cellsig.2024.111258.
50. He, D., Niu, C., Bai, R., Chen, N., and Cui, J. (2024). ADAR1 Promotes Invasion and Migration and Inhibits Ferroptosis via the FAK/AKT Pathway in Colorectal Cancer. Mol Carcinog. 10.1002/mc.23818.
51. Murray, M.B., Leak, L.B., Lee, W.C., and Dixon, S.J. (2023). Protocol for detection of ferroptosis in cultured cells. STAR Protoc *4*, 102457. 10.1016/j.xpro.2023.102457.
52. Leu, J.I., Murphy, M.E., and George, D.L. (2019). Mechanistic basis for impaired ferroptosis in cells expressing the African-centric S47 variant of p53. Proc Natl Acad Sci U S A *116*, 8390-8396. 10.1073/pnas.1821277116.

53. Enache, O.M., Rendo, V., Abdusamad, M., Lam, D., Davison, D., Pal, S., Currimjee, N., Hess, J., Pantel, S., Nag, A., et al. (2020). Cas9 activates the p53 pathway and selects for p53-inactivating mutations. Nat Genet *52*, 662-668. 10.1038/s41588-020-0623-4.
54. Gnanapradeepan, K., Basu, S., Barnoud, T., Budina-Kolomets, A., Kung, C.P., and Murphy, M.E. (2018). The p53 Tumor Suppressor in the Control of Metabolism and Ferroptosis. Front Endocrinol (Lausanne) *9*, 124. 10.3389/fendo.2018.00124.
55. Nagel, R., Semenova, E.A., and Berns, A. (2016). Drugging the addict: non-oncogene addiction as a target for cancer therapy. EMBO Rep *17*, 1516-1531. 10.15252/embr.201643030.
56. Mendez Ruiz, S., Chalk, A.M., Goradia, A., Heraud-Farlow, J., and Walkley, C.R. (2023). Over-expression of ADAR1 in mice does not initiate or accelerate cancer formation in vivo. NAR Cancer *5*, zcad023. 10.1093/narcan/zcad023.
57. Xie, Y., Wang, B., Zhao, Y., Tao, Z., Wang, Y., Chen, G., and Hu, X. (2022). Mammary adipocytes protect triple-negative breast cancer cells from ferroptosis. J Hematol Oncol *15*, 72. 10.1186/s13045-022-01297-1.
58. Ackermann, T., Shokry, E., Deshmukh, R., Anand, J., Galbraith, L.C.A., Mitchell, L., Rodriguez-Blanco, G., Villar, V.H., Sterken, B.A., Nixon, C., et al. (2024). Breast cancer secretes anti-ferroptotic MUFAs and depends on selenoprotein synthesis for metastasis. EMBO Mol Med *16*, 2749-2774. 10.1038/s44321-024-00142-x.
59. Puente-Cobacho, B., Esteo, C., Altea-Manzano, P., Garcia-Perez, J.L., Quiles, J.L., Sanchez-Rovira, P., Martín-Salvago, M.D., Molina-Jiménez, L., Luque, R.J., Fendt, S.-M., and Vera-Ramirez, L. (2024). De novo lipogenesis protects dormant breast cancer cells from ferroptosis and promotes metastasis. Redox Biology, 103480. https://doi.org/10.1016/j.redox.2024.103480.
60. Park, S.Y., Jeong, K.J., Poire, A., Zhang, D., Tsang, Y.H., Blucher, A.S., and Mills, G.B. (2023). Irreversible HER2 inhibitors overcome resistance to the RSL3 ferroptosis inducer in non-HER2 amplified luminal breast cancer. Cell Death Dis *14*, 532. 10.1038/s41419-023-06042-1.
61. Bajbouj, K., Shafarin, J., and Hamad, M. (2019). Estrogen-dependent disruption of intracellular iron metabolism augments the cytotoxic effects of doxorubicin in select breast and ovarian cancer cells. Cancer Manag Res *11*, 4655-4668. 10.2147/CMAR.S204852.
62. Li, X., Rhee, D.K., Malhotra, R., Mayeur, C., Hurst, L.A., Ager, E., Shelton, G., Kramer, Y., McCulloh, D., Keefe, D., et al. (2016). Progesterone receptor membrane component-1 regulates hepcidin biosynthesis. J Clin Invest *126*, 389-401. 10.1172/JCI83831.
63. Liu, L., Zhang, C., Qu, S., Liu, R., Chen, H., Liang, Z., Tian, Z., Li, L., Ma, S., and Liu, X. (2022). ESR1 inhibits ionizing radiation-induced ferroptosis in breast cancer cells via the NEDD4L/CD71 pathway. Arch Biochem Biophys *725*, 109299. 10.1016/j.abb.2022.109299.
64. Wang, H., Hou, M.J., Liao, L., Li, P., Chen, T., Wang, P., and Zhu, B.T. (2024). Strong Protection by 4-Hydroxyestrone against Erastin-Induced Ferroptotic Cell Death in Estrogen Receptor-Negative Human Breast Cancer Cells: Evidence for Protein Disulfide Isomerase as a Mechanistic Target for Protection. Biochemistry *63*, 984-999. 10.1021/acs.biochem.3c00261.
65. Cancer Genome Atlas, N. (2012). Comprehensive molecular portraits of human breast tumours. Nature *490*, 61-70. 10.1038/nature11412.

66. Dibra, D., Xiong, S., Moyer, S.M., El-Naggar, A.K., Qi, Y., Su, X., Kong, E.K., Korkut, A., and Lozano, G. (2024). Mutant p53 protects triple-negative breast adenocarcinomas from ferroptosis in vivo. Sci Adv *10*, eadk1835. 10.1126/sciadv.adk1835.
67. Kung, C.P., and Weber, J.D. (2022). It's Getting Complicated-A Fresh Look at p53-MDM2-ARF Triangle in Tumorigenesis and Cancer Therapy. Front Cell Dev Biol *10*, 818744. 10.3389/fcell.2022.818744.
68. Adams, C.M., Mitra, R., Xiao, Y., Michener, P., Palazzo, J., Chao, A., Gour, J., Cassel, J., Salvino, J.M., and Eischen, C.M. (2023). Targeted MDM2 Degradation Reveals a New Vulnerability for p53-Inactivated Triple-Negative Breast Cancer. Cancer Discov *13*, 1210-1229. 10.1158/2159-8290.CD-22-1131.
69. Cottrell, K.A., Torres, L.S., Dizon, M.G., and Weber, J.D. (2021). 8-azaadenosine and 8-chloroadenosine are not selective inhibitors of ADAR. Cancer Res Commun *1*, 56-64. 10.1158/2767-9764.crc-21-0027.
70. Rehwinkel, J., and Mehdipour, P. (2024). ADAR1: from basic mechanisms to inhibitors. Trends Cell Biol. 10.1016/j.tcb.2024.06.006.
71. Weth, F.R., Hoggarth, G.B., Weth, A.F., Paterson, E., White, M.P.J., Tan, S.T., Peng, L., and Gray, C. (2024). Unlocking hidden potential: advancements, approaches, and obstacles in repurposing drugs for cancer therapy. Br J Cancer *130*, 703-715. 10.1038/s41416-023-02502-9.
72. Lee, J., Lim, B., Pearson, T., Choi, K., Fuson, J.A., Bartholomeusz, C., Paradiso, L.J., Myers, T., Tripathy, D., and Ueno, N.T. (2019). Anti-tumor and anti-metastasis efficacy of E6201, a MEK1 inhibitor, in preclinical models of triple-negative breast cancer. Breast Cancer Res Treat *175*, 339-351. 10.1007/s10549-019-05166-3.
73. Lulli, D., Carbone, M.L., and Pastore, S. (2017). The MEK Inhibitors Trametinib and Cobimetinib Induce a Type I Interferon Response in Human Keratinocytes. Int J Mol Sci *18*. 10.3390/ijms18102227.
74. Jennis, M., Kung, C.P., Basu, S., Budina-Kolomets, A., Leu, J.I., Khaku, S., Scott, J.P., Cai, K.Q., Campbell, M.R., Porter, D.K., et al. (2016). An African-specific polymorphism in the TP53 gene impairs p53 tumor suppressor function in a mouse model. Genes Dev *30*, 918-930. 10.1101/gad.275891.115.
75. Yang, F., Xiao, Y., Ding, J.H., Jin, X., Ma, D., Li, D.Q., Shi, J.X., Huang, W., Wang, Y.P., Jiang, Y.Z., and Shao, Z.M. (2023). Ferroptosis heterogeneity in triple-negative breast cancer reveals an innovative immunotherapy combination strategy. Cell Metab *35*, 84-100 e108. 10.1016/j.cmet.2022.09.021.
76. Bhate, A., Sun, T., and Li, J.B. (2019). ADAR1: A New Target for Immuno-oncology Therapy. Mol Cell *73*, 866-868. 10.1016/j.molcel.2019.02.021.
77. Deng, J., Zhou, M., Liao, T., Kuang, W., Xia, H., Yin, Z., Tan, Q., Li, Y., Song, S., Zhou, E., and Jin, Y. (2022). Targeting Cancer Cell Ferroptosis to Reverse Immune Checkpoint Inhibitor Therapy Resistance. Front Cell Dev Biol *10*, 818453. 10.3389/fcell.2022.818453.
78. Ferrer, M., Mourikis, N., Davidson, E.E., Kleeman, S.O., Zaccaria, M., Habel, J., Rubino, R., Gao, Q., Flint, T.R., Young, L., et al. (2023). Ketogenic diet promotes tumor ferroptosis but induces relative corticosterone deficiency that accelerates cachexia. Cell Metab *35*, 1147-1162 e1147. 10.1016/j.cmet.2023.05.008.

79. Salvadori, G., Zanardi, F., Iannelli, F., Lobefaro, R., Vernieri, C., and Longo, V.D. (2021). Fasting-mimicking diet blocks triple-negative breast cancer and cancer stem cell escape. Cell Metab *33*, 2247-2259 e2246. 10.1016/j.cmet.2021.10.008.
80. Martinez-Garay, C., and Djouder, N. (2023). Dietary interventions and precision nutrition in cancer therapy. Trends Mol Med *29*, 489-511. 10.1016/j.molmed.2023.04.004.

Figure 1

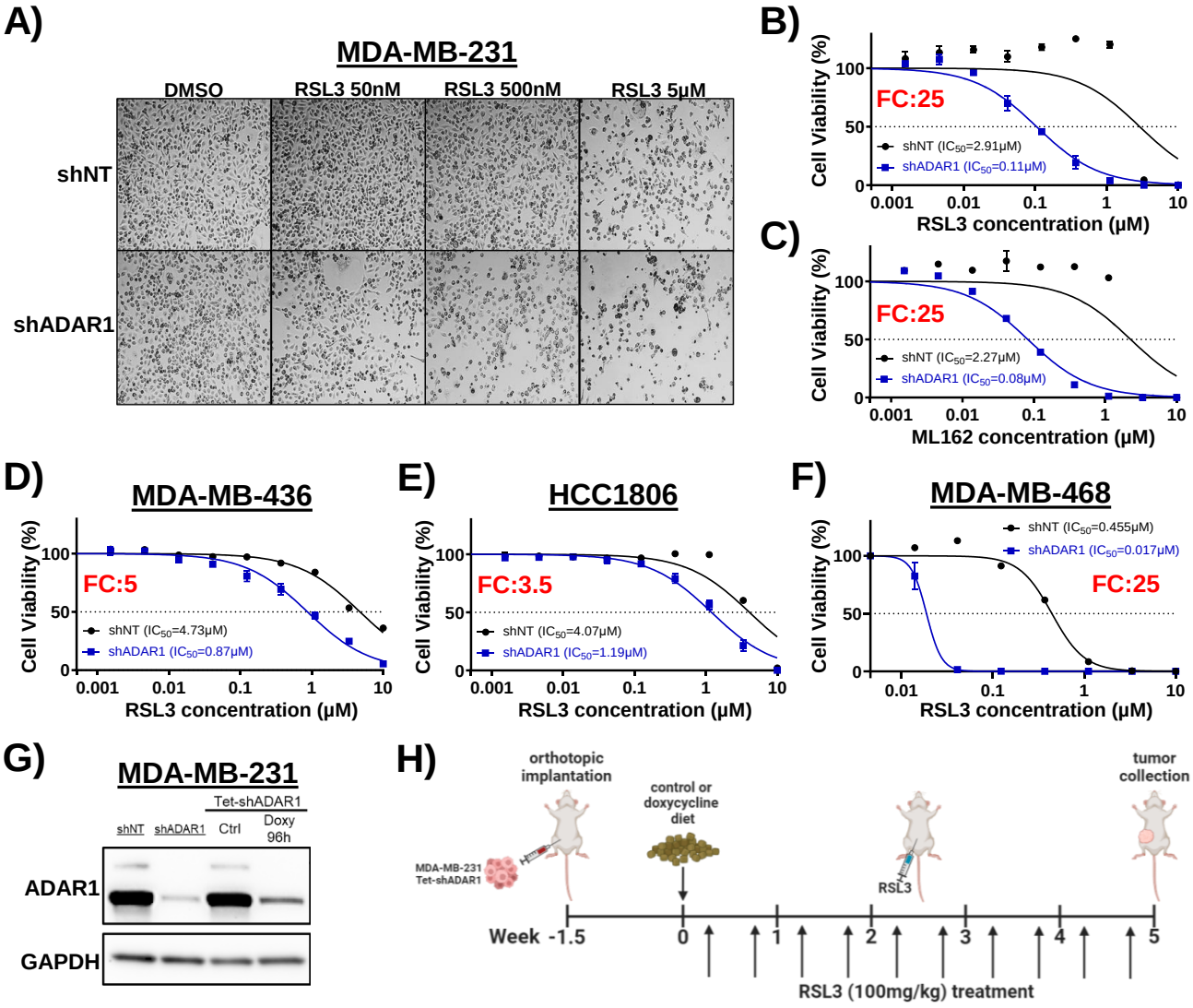

Comparison		p-Value - Post Treatment (Week)					
Group 1	Group 2	0	1	2	3	4	5
Ctrl - Ctrl	Doxy - Ctrl	>0.999	0.957	0.367	**0.015**	**<0.0001**	**<0.0001**
Ctrl - Ctrl	Ctrl - RSL3	>0.999	0.984	0.472	**0.005**	**<0.0001**	**<0.0001**
Ctrl - Ctrl	Doxy - RSL3	>0.999	0.836	0.087	**<0.0001**	**<0.0001**	**<0.0001**
Doxy - Ctrl	Doxy - RSL3	>0.999	0.999	0.963	0.234	0.059	**<0.0001**
Ctrl - RSL3	Doxy - RSL3	>0.999	0.997	0.964	0.606	0.120	**0.002**

Figure 2

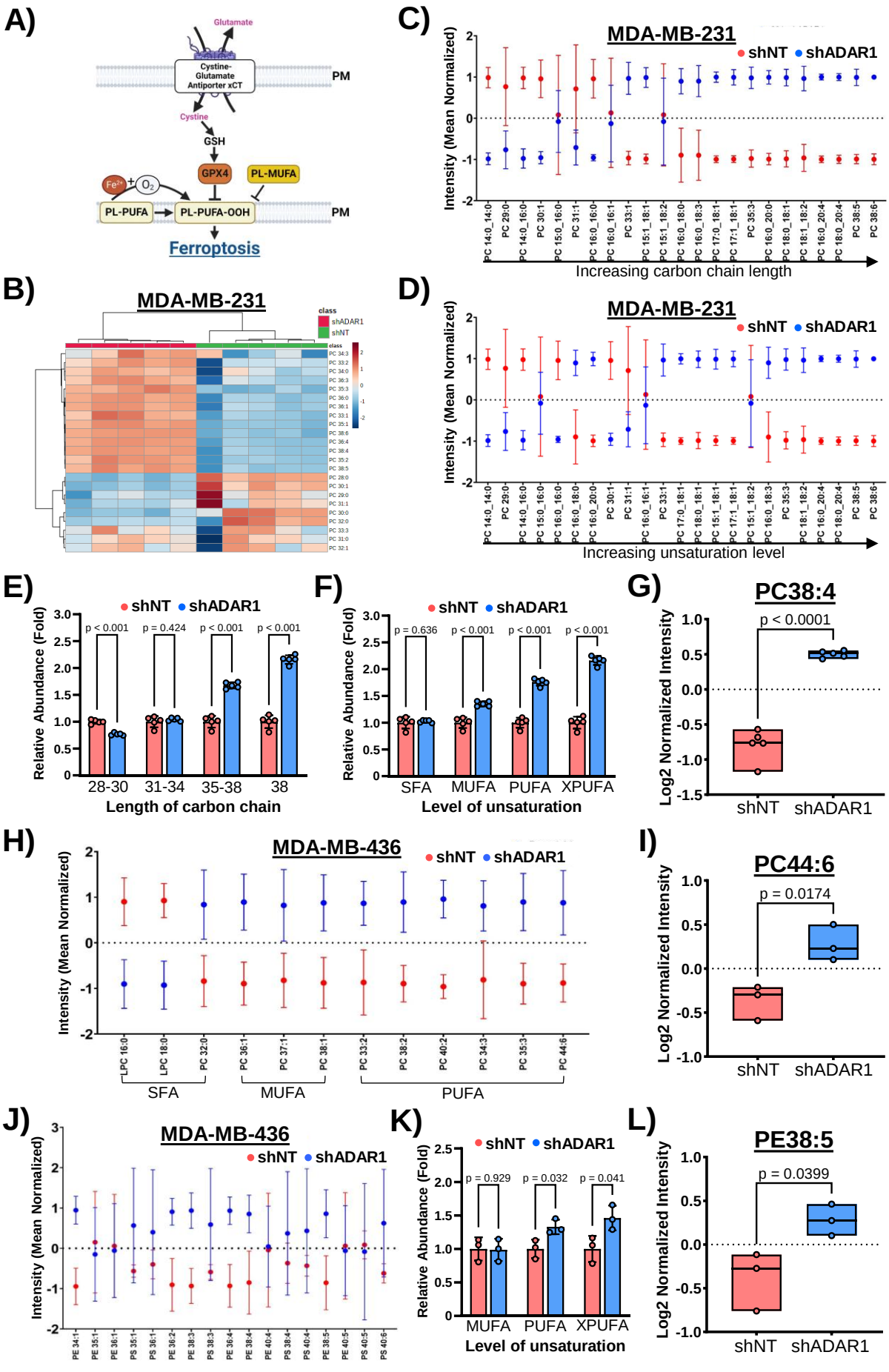
A)
Glutamate
Cystine-Glutamate Antiporter xCT
PM
Cystine
GSH
GPX4
PL-MUFA
PL-PUFA
PL-PUFA-OOH
PM
Ferroptosis
B)
MDA-MB-231
shADAR1
shNT
C)
MDA-MB-231
shNT shADAR1
Intensity (Mean Normalized)
Increasing carbon chain length
D)
MDA-MB-231
shNT shADAR1
Intensity (Mean Normalized)
Increasing unsaturation level
E)
shNT shADAR1
Relative Abundance (Fold)
p < 0.001
p = 0.424
p < 0.001
p < 0.001
28-30
31-34
35-38
38
Length of carbon chain
F)
shNT shADAR1
Relative Abundance (Fold)
p = 0.636
p < 0.001
p < 0.001
p < 0.001
SFA
MUFA
PUFA
XPUFA
Level of unsaturation
G)
PC38:4
p < 0.0001
Log2 Normalized Intensity
shNT
shADAR1
H)
MDA-MB-436
shNT shADAR1
Intensity (Mean Normalized)
SFA
MUFA
PUFA
I)
PC44:6
p = 0.0174
Log2 Normalized Intensity
shNT
shADAR1
J)
MDA-MB-436
shNT shADAR1
Intensity (Mean Normalized)
K)
shNT shADAR1
Relative Abundance (Fold)
p = 0.929
p = 0.032
p = 0.041
MUFA
PUFA
XPUFA
Level of unsaturation
L)
PE38:5
p = 0.0399
Log2 Normalized Intensity
shNT
shADAR1

Figure 3

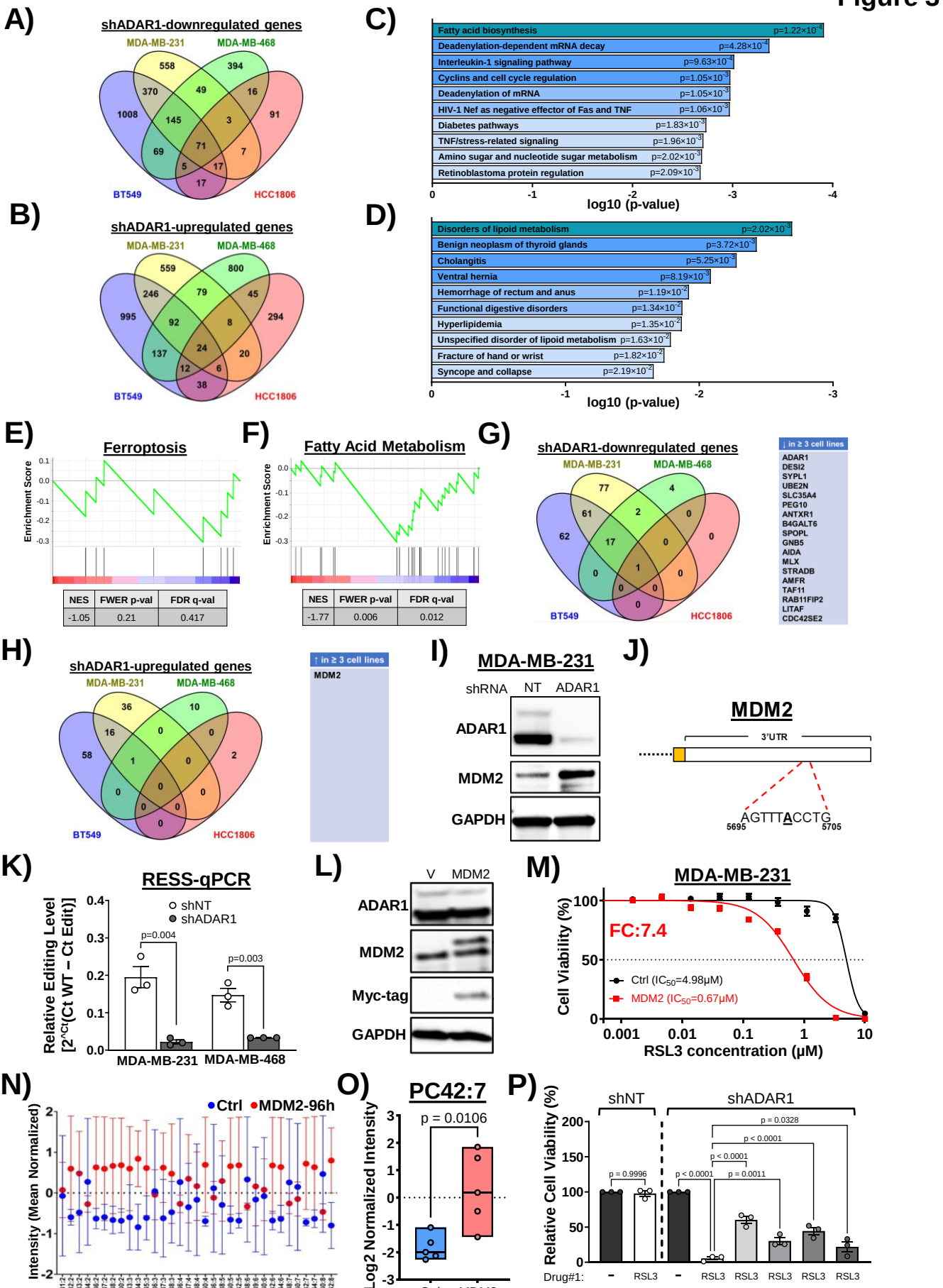
A)
shADAR1-downregulated genes
MDA-MB-231
MDA-MB-468
BT549
HCC1806
558
394
370
49
16
1008
145
3
91
71
69
7
5
17
17
B)
shADAR1-upregulated genes
MDA-MB-231
MDA-MB-468
BT549
HCC1806
559
800
246
79
45
995
92
8
294
24
137
20
12
6
38
C)
Fatty acid biosynthesis p=1.22×10-4
Deadenylation-dependent mRNA decay p=4.28×10-4
Interleukin-1 signaling pathway p=9.63×10-4
Cyclins and cell cycle regulation p=1.05×10-3
Deadenylation of mRNA p=1.05×10-3
HIV-1 Nef as negative effector of Fas and TNF p=1.06×10-3
Diabetes pathways p=1.83×10-3
TNF/stress-related signaling p=1.96×10-3
Amino sugar and nucleotide sugar metabolism p=2.02×10-3
Retinoblastoma protein regulation p=2.09×10-3
0 -1 -2 -3 -4
log10 (p-value)
D)
Disorders of lipoid metabolism p=2.02×10-3
Benign neoplasm of thyroid glands p=3.72×10-3
Cholangitis p=5.25×10-3
Ventral hernia p=8.19×10-3
Hemorrhage of rectum and anus p=1.19×10-2
Functional digestive disorders p=1.34×10-2
Hyperlipidemia p=1.35×10-2
Unspecified disorder of lipoid metabolism p=1.63×10-2
Fracture of hand or wrist p=1.82×10-2
Syncope and collapse p=2.19×10-2
0 -1 -2 -3
log10 (p-value)
E)
Ferroptosis
Enrichment Score
0.1 0.0 -0.1 -0.2 -0.3
NES | FWER p-val | FDR q-val
-1.05 | 0.21 | 0.417
F)
Fatty Acid Metabolism
Enrichment Score
0.0 -0.1 -0.2 -0.3
NES | FWER p-val | FDR q-val
-1.77 | 0.006 | 0.012
G)
shADAR1-downregulated genes
MDA-MB-231
MDA-MB-468
BT549
HCC1806
77
4
61
2
0
62
17
0
0
1
0
0
0
0
0
↓ in ≥ 3 cell lines
ADAR1
DESI2
SYPL1
UBE2N
SLC35A4
PEG10
ANTXR1
B4GALT6
SPOPL
GNB5
AIDA
MLX
STRADB
AMFR
TAF11
RAB11FIP2
LITAF
CDC42SE2
H)
shADAR1-upregulated genes
MDA-MB-231
MDA-MB-468
BT549
HCC1806
36
10
16
0
0
58
1
0
2
0
0
0
0
0
0
↑ in ≥ 3 cell lines
MDM2
I)
MDA-MB-231
shRNA NT ADAR1
ADAR1
MDM2
GAPDH
J)
MDM2
3'UTR
AGTTTACCTG
5695 5705
K)
RESS-qPCR
Relative Editing Level [2^(Ct WT – Ct Edit)]
shNT
shADAR1
p=0.004
p=0.003
0.4 0.3 0.2 0.1 0.0
MDA-MB-231 MDA-MB-468
L)
V MDM2
ADAR1
MDM2
Myc-tag
GAPDH
M)
MDA-MB-231
Cell Viability (%)
100 50 0
FC:7.4
Ctrl (IC50=4.98μM)
MDM2 (IC50=0.67μM)
0.001 0.01 0.1 1 10
RSL3 concentration (μM)
N)
Ctrl MDM2-96h
Intensity (Mean Normalized)
2 1 0 -1 -2
O)
PC42:7
p = 0.0106
Log2 Normalized Intensity
3 2 1 0 -1 -2 -3
Ctrl MDM2
P)
shNT
shADAR1
Relative Cell Viability (%)
200 150 100 50 0
p = 0.0328
p < 0.0001
p < 0.0001
p = 0.9996
p < 0.0001
p = 0.0011
Drug#1: - RSL3 - RSL3 RSL3 RSL3 RSL3 RSL3
Drug#2: - - - - MX69 MEL23 SP141 PA

Figure 4

A)

B)

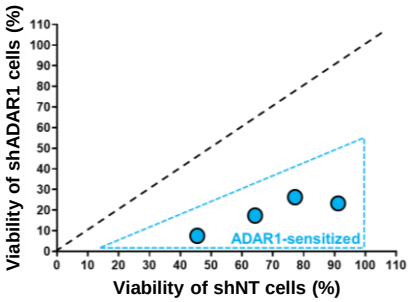

C)

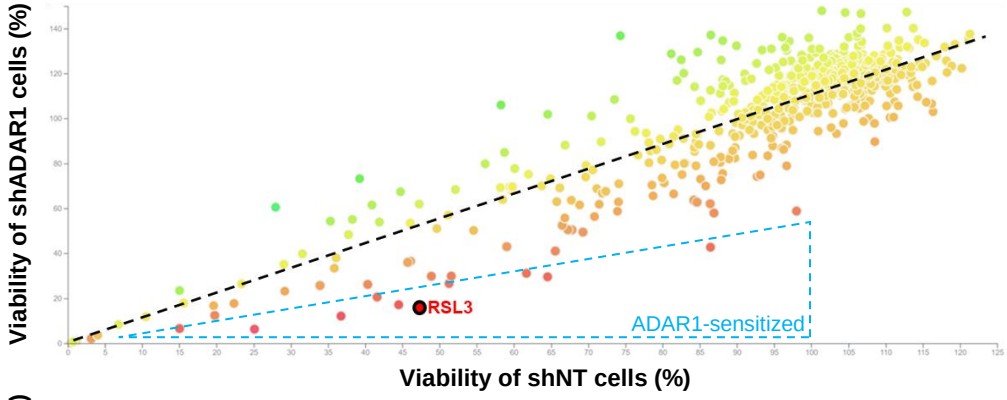

D)

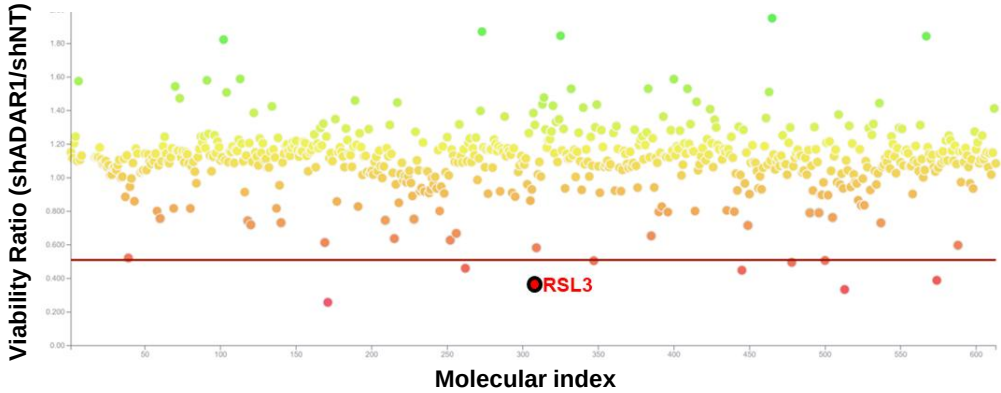

E)

Drug	Viability Ratio (shADAR1/shNT)
Siramesine	0.26
SB-590885	0.33
α-Mangostin	0.39
GW284543	0.45
UC2288	0.46
Nordihydroguaiaretic acid (NDGA)	0.5
Cobimetinib	0.51
Cobimetinib (racemate)	0.51

F)

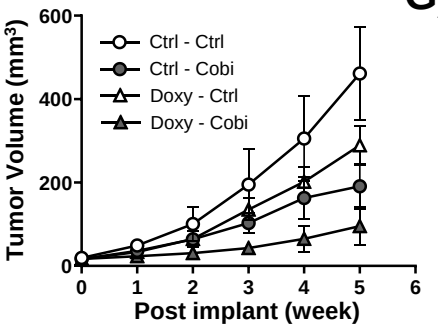

G)

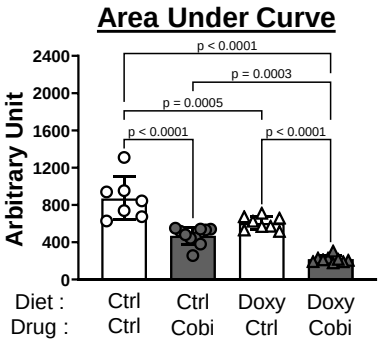

H)

Comparison		p-Value - Post Treatment (Week)					
Group 1	Group 2	0	1	2	3	4	5
Ctrl - Ctrl	Doxy - Ctrl	>0.999	0.957	0.367	0.015	<0.0001	<0.0001
Ctrl - Ctrl	Ctrl - Cobi	>0.999	0.979	0.319	<0.0001	<0.0001	<0.0001
Ctrl - Ctrl	Doxy - Cobi	>0.999	0.725	0.002	<0.0001	<0.0001	<0.0001
Doxy - Ctrl	Doxy - Cobi	>0.999	0.994	0.436	<0.0001	<0.0001	<0.0001
Ctrl - Cobi	Doxy - Cobi	>0.999	0.980	0.426	0.011	<0.0001	<0.0001
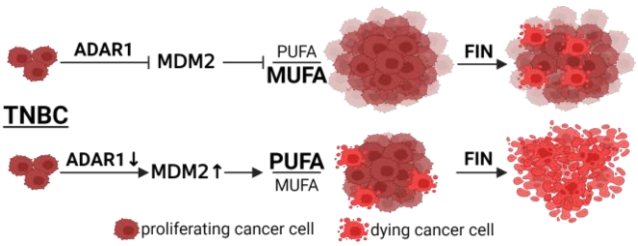
I)